J Food Sci Technol (December 2022) 59(12):4653–4662
https://doi.org/10.1007/s13197-022-05544-8

ORIGINAL ARTICLE

Recombinant protein G/Au nanoparticles/graphene oxide modified electrodes used as an electrochemical biosensor for *Brucella* Testing in milk

Hongshuo Chen[1,3] · Haibin Liu[2] · Chuanjin Cui[1] · Wensi Zhang[1] · Yueming Zuo[3]

Revised: 14 June 2022 / Accepted: 19 June 2022 / Published online: 9 July 2022

Abstract In this study, a simple label-free biosensor for *Brucella* was constructed, which based on the screen-printed carbon electrode (SPCE) modified by Recombinant protein G/gold nanoparticles/graphene oxide (RpG/Au/GO). The impedance responses of the proposed biosensor were measured by electrochemical AC impedance method in *Brucella* antigen gradient concentration solutions. The results showed that the linear range of this biosensor was from 1.6×10^2 CFU/mL to 1.6×10^8 CFU/mL with the minimum detection limit of 3.2×10^2 CFU/mL (S/N = 3). Moreover, the biosensor for *Brucella* detection possessed acceptable reproducibility with a relative standard deviation of 5.15% and acceptable stability with a relative standard deviation of 4.68%. The spiked recovery rate in actual pasteurized milk samples was more than 92%. Therefore, the developed biosensor exhibits excellent prospects in the selective quantification detection of *Brucella abortus*.

Keywords Brucella · Recombinant protein G · Screen-printed carbon electrode · Biosensor

Abbreviations

SPCE	Screen-printed carbon electrode
RpG	Recombinant protein G
Au	Gold nanoparticles
GO	Graphene oxide
CV	Cyclic voltammetry
EIS	Electrochemical impedance spectroscopy
Rct	Charge transfer resistance
XRD	X-ray diffraction
SPR	Surface Plasmon resonance

Introduction

Brucellosis is a significant zoonotic disease, and the infected animals or animal products are the primary sources of human infection. Brucellosis usually causes abortion and animals sterility, which will cause not only huge economic losses to the animal husbandry but also a severe threat to public health safety (Robi and Gelalcha 2020).Therefore, the early detection of Brucellosis is vital to control its spread.

Brucella immunoassay techniques include the rose bengal plate test (RBPT), standardized agglutination test (SAT), and PCR methods (YENİ and Doğan 2021). Thereinto, RBPT and SAT are the gold standards for *Brucella* detection. However, they have some shortcomings during testing, such as high risk, time-consuming, and the requirement of a biosafety level 3 laboratory (Sabour et al. 2020). PCR methods have good specificity and high sensitivity for routine tests (Satei et al. 2020) but have significant limitations related to the requirement of qualified personnel and expensive equipment, among others. Electrochemical biosensors have emerged as outstanding analytical tools for microbial detection by combining biosensing and electrochemical analysis technology (Zhang et al. 2022). Moreover, it

Supplementary Information The online version contains supplementary material available at https://doi.org/10.1007/s13197-022-05544-8.

✉ Hongshuo Chen
chs@ncst.edu.cn

[1] College of Electrical Engineering, North China University of Science and Technology, Tangshan 063210, People's Republic of China

[2] College of Life Sciences, North China University of Science and Technology, Tangshan 063210, People's Republic of China

[3] College of Engineering, Shanxi Agricultural University, Taigu 030801, People's Republic of China

possesses significant advantages, such as robustness, excellent detection limits, a wide range of responses, low sample volume need and easy miniaturization (Pérez-Fernández and de la Escosura Muñiz 2022). So it has played an important role in food safety testing, drug analysis, health care, and environmental monitoring (Bayramoglu et al. 2019; Wahab et al. 2017).

Graphene oxide (GO) is an oxidized form of graphene laced with oxygen-containing groups, such as epoxide, carboxyl, and hydroxyl functional groups on the carbon surface(Chang et al. 2022). It has been applied for the construction of electrochemical biosensors because of its large surface-to-volume ratio, good electrical conductivity and excellent biocompatibility (Gao et al. 2022a; Li and Tang 2011; Zhang et al. 2019). Nanogold has been used for biological and chemical detections and analytical applications due to its simple preparation, high specific surface area, high electrical conductivity and biocompatibility (Chauhan et al. 2020; Zhao et al. 2021). In addition, nanogold can provide a friendly microenvironment for bioelectrocatalysis, and be a conductive channel. So it is easy to achieve direct electron transfer between analyte and electrode (Huang et al. 2016; Zhao et al. 2014).

Self-assembled monolayer (SAM) technology is a nanoscale membrane preparation technology based on charge forces, hydrogen bonding forces, charge transfer and host–guest interactions. It has been used to address electroanalytical challenges. (Love et al. 2005; Ulman 1996; Zhao et al. 2014). During antibody immobilization, there were some problems such as large spatial site resistance, easy inactivation of antibody, and low efficiency. So the technique of oriented antibody coupling attracted the attention of researchers to solve them (Gao et al. 2022b). Protein A and protein G are specific antibody-binding proteins which can be used to regulate the localization of full-length antibodies (Guang-Feng et al. 2013; Yin et al. 2018). Protein A and protein G have been proved to be a good intermedium. They are commonly used for the targeted immobilization of antibodies to improve the detection range and the detection limit of the biosensor (Moon et al. 2019; Wang et al. 2020). Significantly, the IgG-binding domains on proteins A and G may selectively adsorb the Fc regions of various antibodies and do not interfere with antibodies' binding specificity, making them the optimal candidate interlayer for biosensors (Dong et al. 2015; Yin 2019). It is already known that nanogold can enhance protein adsorption, so Au–S bonds are often used to bind biomolecules during biosensor preparation (Malathi et al. 2022). Recombinant protein G (RpG) equipped with a sulfhydryl group (-SH) at the carbon terminus can form a gold-sulfur bond with nanogold. Compared with protein A, RpG has a higher affinity for most IgG and can reduce cross-reactivity and non-specific binding because it removes the binding sites of albumin and cell surfaces (Chammem et al. 2015; Liu et al. 2019). Therefore, recombinant protein G is more applicable as the intermedium of antibody immobilization.

In this study, we attempted to obtain a biosensor for Brucella testing with higher precision, a wider detection range and a lower detection limit. Its construction was based on the following technology, such as the oriented immobilization for antibodies of the recombinant protein G and the outstandingly synergistic effect between graphene oxide and nanogold. The electrochemical impedance spectroscopy (EIS) of the proposed biosensor was tested in a series of concentrations of *Brucella* solution. The fabrication process of the biosensor is exhibited in Fig. 1.

Material and methods

Materials and chemicals

Brucella-primary antibody, *Brucella* Antigen (1.6×1011 CFU/mL) and *Brucella* Negative Serum were purchased from the China Veterinary Drug Control Institute. Heat-inactivated *E. coli* (O157:H7) and *Staphylococcus aureus* were provided by School of Basic Medical Sciences, North China University of Science and Technology. Recombinant protein G was purchased from Shanghai Ya Xin Biotechnology Co., LTD. Graphene oxide was purchased from Nanjing Xian Feng Nanomaterials Technology Co., LTD. Chloroauric acid ($HAuCl_4\ 4H_2O$), potassium ferricyanide ($K_3Fe\ (CN)_6$), potassium ferrocyanide ($K_4Fe\ (CN)_6$), 0.01 M phosphate buffer saline (PBS) and other reagents were purchased from Aladdin (China). All used chemical reagents were of analytical reagent grade without further purification. Ultrapure water (> 18.2 MΩ) was obtained from a PINETREE purification system in the experiment.

Apparatus and measurements

Field emission Scanning electron microscope (Thermo Fisher Technology Co., LTD, Czech Republic) was used for the characterization of the prepared nanomaterials. The X-ray diffractometer (Rigaku Corporation, Japan) was conducted to study the crystallite phase with a CuKa (1.5406 A°) radiation source within 5°–90° range of 2θ scale at room temperature.

Gamry reference 600 workstation (Gamry Electrochemical Instruments Inc, America) was applied to perform the electrochemical testing. Screen-Printed carbon electrode (SPCE) was purchased from Spain DRS Technologies, Co., LTD, with a Working electrode: Carbon (4 mm diameter), Auxiliary electrode: Carbon, and Reference electrode: Silver. All electrochemical measurements were carried out in

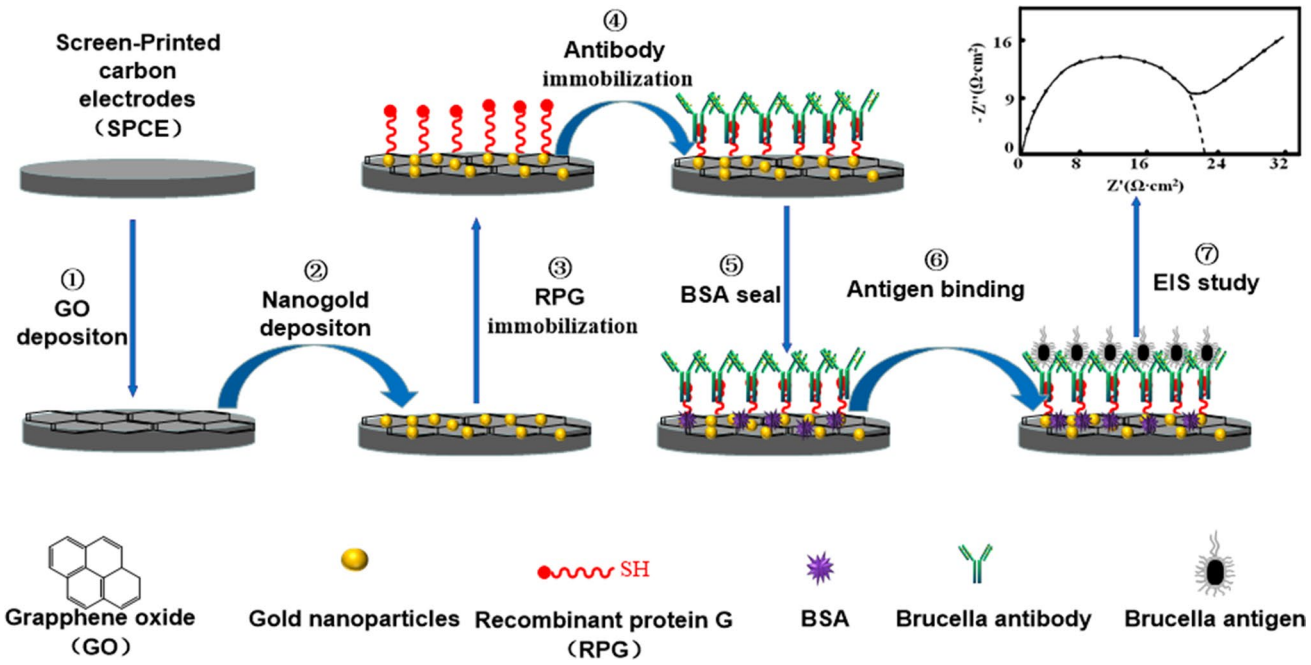

Fig. 1 Schematic illustration of the stepwise assembly of the biosensor for *Brucella*

electrolytes containing 5 mM $Fe(CN)_6^{3-}/Fe(CN)_6^{4-}$ and 0.1 M KCl.

The preparation of the GO/SPCE

Graphene oxide films were prepared using a modified method (Chen et al. 2011). Weighed Graphene oxide powder, dispersed it with PBS solution (0.067 mol/L, pH = 9.18), and sonicated continuously for 2 h under ice bath conditions to ultimately form 1 mg/mL graphene oxide. The electrodeposition conditions: 4 °C, scanning voltage −1.5 V to 0.5 V and scanning speed 25 mV/S. The modified electrode was named as GO/SPCE.

The preparation of the Au/GO/SPCE

The nanogold modification layers were prepared using an improved method (Hezard et al. 2012). Dissolved $HAuCl_4$ $4H_2O$ solid into 0.1 mol/L KNO_3 solution to get Au ion solution (0.5 mmol/L), and then electrodeposited on the GO/SPCE from 0 V to 0.9 V with a scanning speed of 25 mV/S at 4 °C. The Au/GO/SPCE was gained.

The preparation of the RpG/Au/GO/SPCE

RpG freeze-dried powder was dissolved into 1 mL PBS solution (10 mmol/L, pH = 7.4), and then tris(2-carboxyethyl) phosphine hydrochloride was added to make its final concentration to 1 mmol/L. 15 µL RpG solution was added dropwise to the working area of Au/GO/SPCE and incubated at 37 °C for 1 h to generate SAM of RpG. The modified electrode was named as RpG/Au/GO/SPCE.

Sensor testing

50 uL *Brucella* antibodies (0.05 mg/mL), 15 µL 0.5% BSA in PBS solution (w/v, to prevent non-specific reaction) and 50 µL antigen solution was added in sequence on the RpG/Au/GO/SPCE, and incubated at 37°C for 30 min. After each step, the electrode surface should be rinsed with 10 mmol/L PBS buffer and ultrapure water and be dried naturally. Impedance test for biosensor was performed between 0.1 and 10^5 HZ.

Results and discussion

Cyclic Voltammetry characterization during the biosensor preparation process

Cyclic Voltammetry (CV) is a convenient and effective method used to obtain information about electrochemical procedures (Jafari-Kashi et al. 2022). Therefore, the electrochemical behavior of the proposed biosensor preparation process was evaluated using CV measurements (Fig. 2a). The oxidation peak current was calculated and listed in Table S1. The results showed the peak current increased from 117.04 µA (bare SPCE) to 133.3 µA after

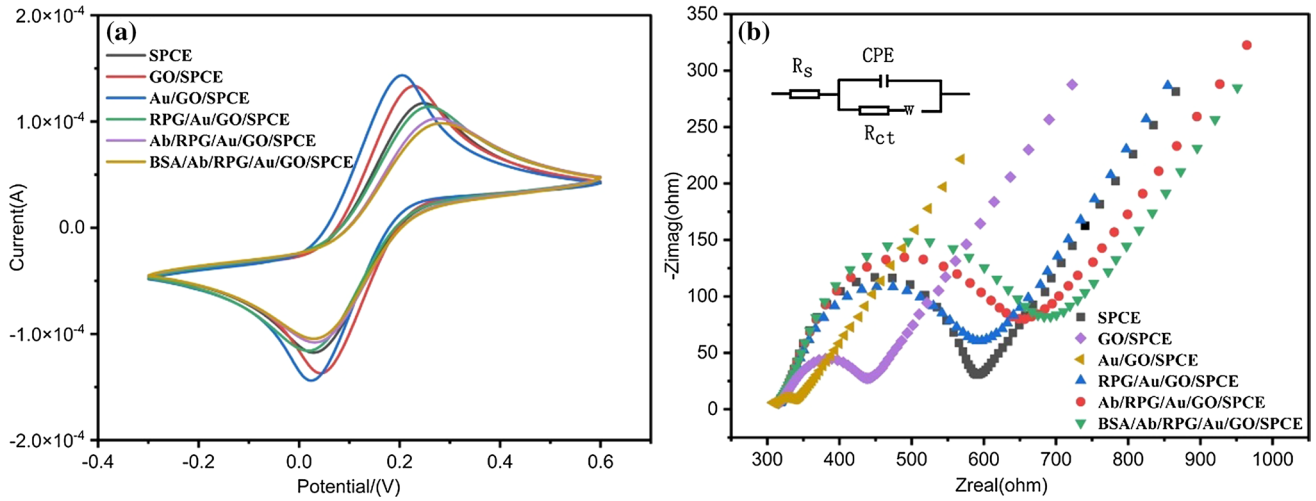

Fig. 2 **a** CV and **b** EIS characterization of the preparation process of the biosensor for *Brucella* (inset image: equivalent circuit diagram)

graphene oxide deposition, and the peak current increased to 143.50 μA after gold nanoparticles electrodeposition. The peak current of SPCE, GO/SPCE and Au/GO/SPCE were brought into Eq. (1), and the electroactive areas were found 0.1411 cm^2, 0.1607 cm^2 and 0.1730 cm^2, respectively. The results indicated that the modification of graphene oxide and nanogold increased the electrode's active area and enhanced the electrochemical response in $[Fe(CN)_6]^{4-/3-}$ solution.

$$I_{pa} = \left(2.69 \times 10^5\right) n^{3/2} C A D^{1/2} V^{1/2} \quad (1)$$

where I_{pa} is the anode peak current (A), n is the electron transfer number, C is the $[Fe(CN)_6]^{4-/3-}$ concentration (moL/cm^3), A is the electrode active surface area (cm^2), D is the solution $[Fe(CN)_6]^{4-/3-}$probe diffusion coefficient (7.6×10^{-6} cm^2/s) and V is the scan rate (V/s).

Nevertheless, the peak current began to decrease orderly when the modified electrode was successively coated with RpG, *Brucella* Ab and BSA, which indicated the modified electrode was covered with a layer-by-layer biofilm hindering the electron transfer rate on the electrode surface (Chen et al. 2020).

Electrochemical impedance spectroscopy characterization during the biosensor preparation

Electrochemical impedance spectroscopy (EIS) was regarded as a potent tool for studying the surface characterization of biosensors. In the Nyquist plot, the semicircle under the higher frequency is correlated with charge transfer resistance (Rct). A linear part under lower frequency corresponds to the diffusion-limited process (Wang et al. 2019). Hence, to further study the surface characteristics of the prepared biosensors, EIS measurement also was applied in this paper (Fig. 2b), and the charge transfer resistance (Rct) was calculated (Table S2). It can be seen that the Rct values become gradually smaller with the subsequent electrodeposition of graphene oxide and nano-gold, which is consistent with the CV variation law. However, the Rct value increased directly from 52.62 to 261.09 Ω after RpG modification and increased sequentially to 322.83 Ω and 355.37 Ω with the immobilization of *Brucella* antibody and BSA. This result confirmed the formation of a biological complex layer and inhibited electron transfer of the biosensor surface (Yuan et al. 2018).

Scanning electron microscopy characterization

Knowing the microstate changes of the electrode surface is helpful for further studying the kinetic process and electrochemical reaction process of the electrode. Furthermore, scanning electron microscope is regarded as a powerful tool for observing the material surface (Smith and Oatley 1955). Therefore, the surface of the biosensor was evaluated to illustrate the size and morphology of the as-prepared nanomaterials. Figure 3a showed that the surface of bare SPCE is convex and uneven, attached much flaky carbon and carbon powder particles. The surface of GO/SPGE was covered with a thin film substance like the unique folded shape of GO, consistent with our previous work (Chen et al. 2020). This result indicated the successful electrodeposition of GO on the SPCE (Fig. 3b). Then we also observed a large amount of uniformly distributed granular material of about 50 nm on the surface of graphite oxide after the nanogold electrodeposition (Fig. 3c). In addition, EDS energy spectrum was employed to analyze the chemical composition of the nanocomposites on the Au/GO/SPCE. Figure S1 showed

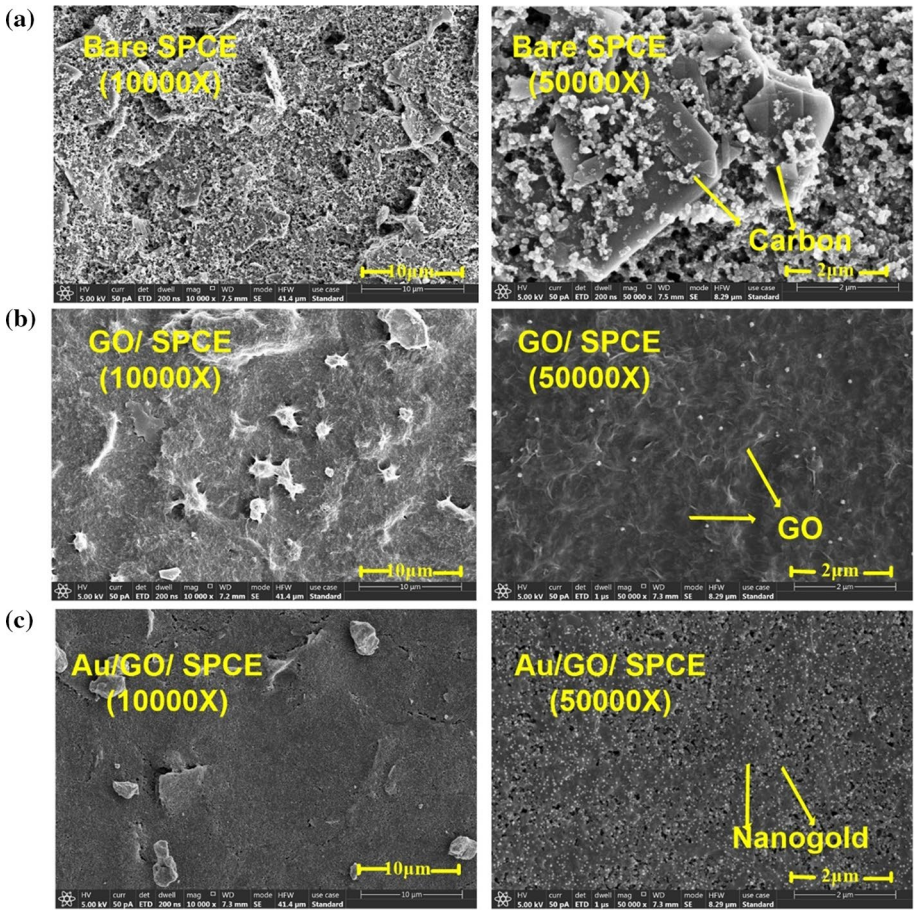

Fig. 3 The SEM of **a** bare SPCE, **b** GO/SPCE and **c** Au/GO/SPCE

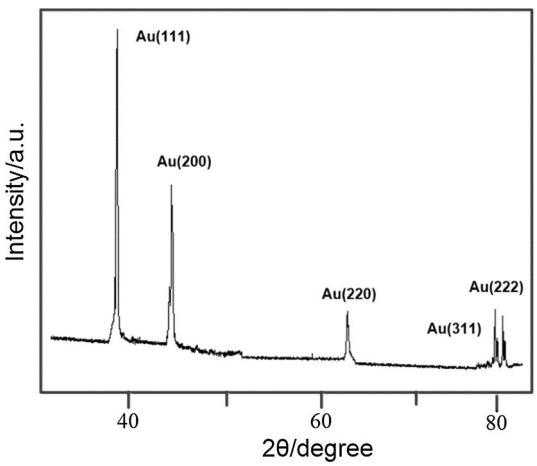

Fig. 4 The XRD of the nanogold

the mass percentage of Au elements reached 10.50%, which confirmed the successful preparation of the gold nanoparticles by electrochemical method (Fig. 4).

X-ray diffraction characterization

X-ray diffraction (XRD), as an category of nondestructive testing, has become an essential tool for microstructure analysis of nanomaterials (Yuan 2014). Hence, XRD was employed to study the crystallinity of the gold nanoparticles on the modified SPCE. Nanogold presented the diffraction patterns at 38.7°, 44.8°, 64.5°, 77.7° and 81.8° with the miller indices of (111), (200), (220), (311) and (222), respectively. Moreover, the maximal peak intensity was near $2\theta = 38.7°$, indicating the growth of nanogold crystal nucleus was mainly in the (111) direction. It was consistent with the reported crystal type (De Lima et al. 2020). This result further confirmed the successful electrodeposition of gold nanoparticles.

Optimization of experimental conditions

Number of the graphene oxide deposition

Graphene oxide with a large specific surface area can increase the effective area of the electrode surface, which is the main factor affecting the performance of the prepared biosensor. For obtaining a more well biosensor, the deposit

quantity of GO was studied by the CV method. Figure S2a exhibited that when the deposition turn was longer than 6, the peak current began to be stable, suggesting that the amount of GO deposited on the sensor's surface reached optimum value. More amount of GO cannot further improve the conductivity of the electrode because graphene accumulation is unfavorable to the electron transfer. Therefore, we chose 6 turns as the optimum parameter.

Number of the chloroauric acid deposition

Immobilizing the biological substance on the surface of SPCE by the Au–S bond is a simple and effective method, then loading appropriate amounts of gold nanoparticles on the surface of GO is the essential step for preparing the modified electrode (Dca et al. 2022). Therefore, the deposition quantity of gold nanoparticles was investigated to improve the sensitivity of the biosensor and provide a favorable platform for immobilizing RpG.

As shown in Fig. S2b, the peak current increased rapidly with the increasing deposition turns from 2 to 4. However, the peak current decreased when the deposition reached 6 turns, which should be attributed to the uneven accumulation of the nanogold hindering the surface electron transfer. Consequently, 4 turns were selected as the optimal electrodeposition parameter of the nanogold.

Recombinant protein G incubation concentration

Antibody density is an important factor affecting antigen-binding efficiency, so we may achieve good antibody immobilization by adjusting the SAM amount of the RpG. Figure S2c showed that the semicircle diameter in the Nyquist plots gradually enlarged with the increase of RpG concentration, indicating the electrode surface was covered with more RpG. However, the semicircle diameter had no significant change when the concentration reached 1.0 mg/mL. Hence, 0.6 mg/mL was regarded as the optimal concentration parameter.

Antibody incubation time

The incubation time is a crucial parameter affecting antibodies' oriented immobilization quantity through RpG. Furthermore, it requires some time to coordinate of the Fc regions of antibody to the binding domains of RpG. Therefore, the fabricated biosensor was incubated with *Brucella* antibody for a certain time (15 min, 30 min, 45 min, 60 min, 75 min) to obtain the optimal response signal. The relationship between incubation time and the impedance change ΔZ was established as the following formula:

$$\Delta Z = R_{Ag} - R_{BSA} \tag{2}$$

where R_{Ag} represents the R_{ct} after binding the *Brucella* antigen (1.6×10^4 CFU/mL), and R_{BSA} represents the R_{ct} after being closed by blocker BSA. As shown in Fig. S2d, the ΔZ increased from 110.80 to 137.68 Ω when the incubation time reached from 15 to 30 min. Nevertheless, when the incubation time was longer than 30 min, the ΔZ remained equable. Therefore, we chose 30 min as the optimal incubation time.

Detection and Analysis of *Brucella* biosensors

Impedance in various concentrations of the Brucella solutions under the optimal conditions were tested to evaluate the performance of the prepared biosensor. It can be seen from the Nyquist plot (Fig. 5a) the semicircular arc diameter (R_{ct}) gradually increased with the increase of the *Brucella*

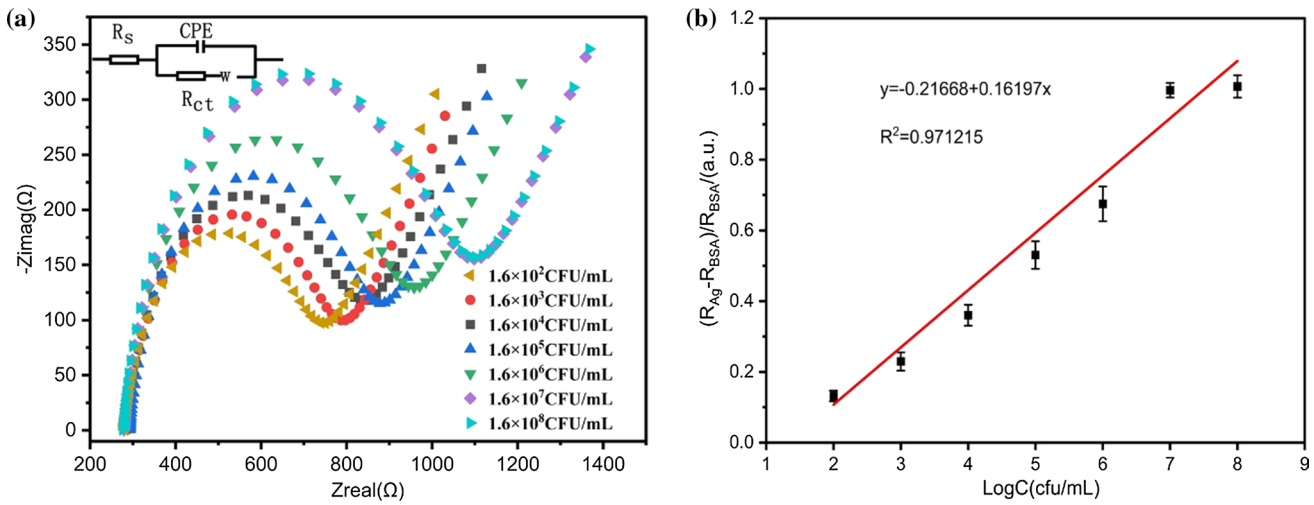

Fig. 5 **a** Nyquist plot and **b** Calibration curve of the biosensor for *Brucella*

solution concentration, which only reflects the relationship between the real and imaginary parts of the impedance. The phenomenon indicated more antibody-antigen complexes generated and covered the surface of the biosensor, and then hindered the charge transfer rate of the biosensor surface. Moreover, we fit the data and built an equivalent circuit (inset, Fig. 5a). The solution impedance (R_s) was 282.58 ± 5.65Ω (RSD = 1.98%) when the antigen concentrations were in the range of 1.6×10^2 CFU/mL to 1.6×10^8 CFU/mL. This result confirmed that the value of the R_s was almost unaffected by the generation of antibody-antigen complexes.

Meanwhile, we also studied the bode plot (Fig. S3). It could be seen that the impedance modulus increased gradually with the increase of antigen concentration only at low-frequency conditions (Fig. S3a). In contrast, phase angle was positive correlation with the antigen concentration when the frequency logarithm is 1 to 2.5. In sum, the bode plot well reflected the integrated characteristics of resistance and capacitance, thus indicating our model accorded with the electrode surface response law.

The calibration curve was built using the logarithm of the antigen concentration as the horizontal coordinate and the dimensionless Ź as the vertical coordinate. (Fig. 5b). The $\acute{Z}$ value (refer to formula 3) can reduce the variation between electrodes and make the data more scientific and reasonable. The results revealed that the logarithm of the antigen concentration (from 1.6×10^2 to 1.6×10^8 CFU/mL) positively correlated with the Ź value. The linear equation was $y = -0.21668 + 0.16197\times$, the linear correlation coefficient R = 0.9855, and the lowest detection limit (S/N = 3) was 3.2×10^2 CFU/mL. The remarkable performance of biosensors should be attributed to the excellent orientation immobilization of the *Brucella* antibody, and the synergetic signal amplification effect of GO and nanogold.

$$\acute{Z} = \left(R_{Ag} - R_{BSA}\right)/R_{BSA} \tag{3}$$

where R_{BSA} and R_{Ag} denote, respectively, the charge transfer impedance of the proposed biosensor after BSA sealing and antigen-binding.

Compared with the previously reported biosensors (Table. S4), the proposed biosensors obtained a satisfactory result with an upper limit of detection of 10^8 CFU/mL and a lower limit of detection of 10^2 CFU/mL. The upper limit of detection was 1–2 orders of magnitude higher than other electrochemical biosensors, and the lower limit of detection was comparable to SPR immunoassay. This result should be attributed to the generating of GO and Au nanocomposites. Its property was superior to the reported nanomaterials, such as onefold gold nanoparticles (Wu et al. 2013), Cu doped NiO and ZrO_2 (Khan et al. 2018), and Cu doped MgO (Khan et al. 2017) that were used for the preparation of sensors of *Brucella* detection. Therefore, we confirmed that a novel ultra-sensitive biosensor was successfully obtained.

Specificity test of the biosensor

Specificity is an essential indicator in evaluating the performance of biosensors. Heat-inactivated *Staphylococcus aureus* (1.0×10^9 CFU/mL) and Escherichia *coli O157:H17* (4.0×10^9 CFU/mL) were used as interfering bacteria to verify the specificity of the proposed biosensor. The impedance change of the biosensor were tested. The results showed there was a significant difference ($p < 0.01$) between the impedance change of interfering bacteria and *Brucella abortus*, and there was not a significant difference ($p > 0.05$) between the impedance change of interfering bacteria and the blank group. This result confirms that the prepared biosensor has acceptable specificity for *Brucella abortus* (Fig. 6a).

Reproducibility test of the biosensor

"Good reproducibility" means the prepared biosensors in the same conditions do not cause unacceptable determination results due to the biosensor's bias. Five biosensors were prepared using the same method, and their impedance change was tested in a 1.6×10^5 CFU/mL *Brucella* antigen solution. The results showed that the minimum impedance (154.39 Ω) for the prepared biosensors was 93.03% of the maximum impedance change (165.95 Ω), and the RSD for the five biosensors was 3.15% (n = 3). Therefore, we deemed the reproducibility of the biosensors acceptable (Fig. 6b).

Stability test of the biosensor

As another indicator of the biosensor, stability is also vital for the real sample detection. Rapid detection and analysis have become a tendency in the field of detection nowadays. Hence, biosensors need to be prepared ahead of time, and their storage time should be studied to acquire outstanding performance. A series of biosensors were fabricated simultaneously and then stored at 4 °C. Figure 6c showed the impedance responses appeared to have an overall decreasing trend as time passed, which was related to the loss of antibody activity during storage. After 10 days, the impedance responses of these biosensors were at 90.60% of the initial impedance response. Moreover, the RSD for the stability test of the biosensor is 4.68% (n = 3). The results confirmed that this fabricated biosensor had good stability.

Detection of actual pasteurized milk simples

Brucella abortus exists in the serum, raw milk or incompletely sterilized milk of infected cattle. Pasteurized

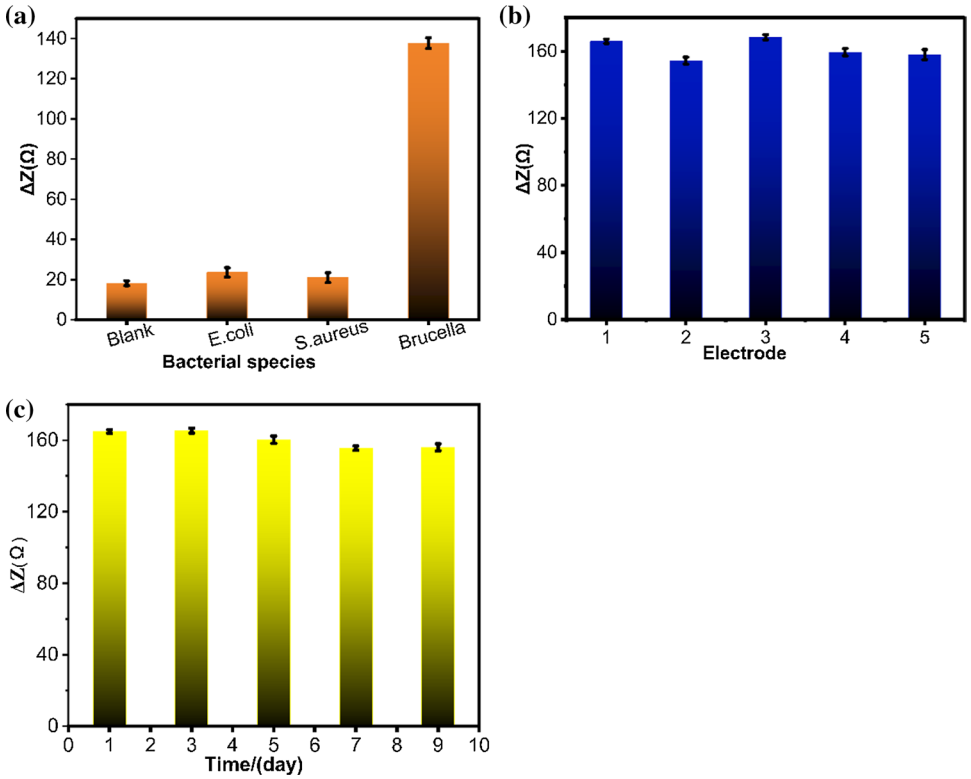

Fig. 6 **a** Specificity, **b** Reproducibility and **c** Stability test of the biosensor for *Brucella* (Error bars represent mean ± SD, where n = 3 replicates)

milk was spiked with high (1.6×10^8 CFU/mL), medium (1.6×10^5 CFU/mL) and low (1.6×10^2 CFU/mL) concentrations of *Brucella abortus*, and then the constructed biosensor was applied for the spiked recovery test. The spiked recoveries were calculated with the averages of three replicates according to Eq. (4). The recoveries of the three concentrations were 92.97%, 98.79% and 100.71%, and the RSDs were 5.40%, 1.51% and 3.6%, respectively. The above results suggested that the proposed sensor assay can identify the *Brucella abortus* in Pasteurized milk samples with a minimum concentration of 1.6×10^2 CFU/mL and a maximum concentration of 1.6×10^8 CFU/mL. (Table S3).

$$M(\%) = \left[1 - (A - B)/B\right] \times 100\% \quad (4)$$

where M is the recovery (%), A is the spiked measurement value (CFU/mL), B is the spiked amount (CFU/mL).

Conclusion

In conclusion, a unique biosensor has been developed for the highly selective and sensitive detection of *Brucella*. The RpG/Au/GO/ /SPCE biosensor integrated the synergistic conductivity ability of GO and gold nanoparticles and the high selectivity of RpG property for *Brucella* antibody. Moreover, the RpG/Au/GO/SPCE biosensor exhibited excellent anti-interference capability, reproducibility and stability, which can be regarded as a reliable method for the rapid determination of *Brucella*. At optimum conditions, the RpG/Au/GO/SPCE presented high sensitivity for *Brucella* within the concentration range 1.6×10^2–1.6×10^8 CFU/mL with a detection limit of 3.2×10^2 CFU/mL (S/N = 3). Furthermore, the RpG/Au/GO/SPCE biosensor was applied successfully to test *Brucella* in Pasteurized milk samples with acceptable recovery data of 92.97–100.71%. As far as we know, there are not many studies on electrochemical biosensors for *Brucella* detection. Moreover, the performance of the developed electrochemical biosensor in this study was satisfactory. Hence, it can be concluded that the proposed biosensor can be applied as a new tool for detecting *Brucella abortus*.

Acknowledgements Thanks to Professor Yueming Zuo for language help in this article.

Funding Our work has been supported by several organizations. We are sincerely grateful for the financial support from the Project of Youth Fund for Science and Technology Research in Hebei Universities (Grant number: QN2020194), the Project of Youth Fund for National Natural Science Foundation of China (Grant number: 32001791) and the National Natural Science Foundation of China (Grant number 30871445).

Declarations

Conflicts of interest The authors declare no conflict of interest.

Ethics approval Not applicable.

References

Bayramoglu G, Ozalp VC, Oztekin M, Arica MY (2019) Rapid and label-free detection of *Brucella* melitensis in milk and milk products using an aptasensor. Talanta 200:263–271. https://doi.org/10.1016/j.talanta.2019.03.048

Chammem H, Hafaid I, Bohli N, Garcia A, Meilhac O, Abdelghani A, Mora L (2015) A disposable electrochemical sensor based on protein G for high-density lipoprotein (HDL) detection. Talanta 144:466–473. https://doi.org/10.1016/j.talanta.2015.06.009

Chang YJ, Lee MC, Chien YC (2022) Quantitative determination of uric acid using paper-based biosensor modified with graphene oxide and 5-amino-1, 3, 4-thiadiazole-2-thiol. SLAS Technol 27(1):54–62

Chauhan P, Raja AN, Jain R (2020) Nanogold modified glassy carbon sensor for the quantification of phytoestrogenchlorogenic acid. Surf Interf 19:100536

Chen L, Tang Y, Wang K, Liu C, Luo S (2011) Direct electrodeposition of reduced graphene oxide on glassy carbon electrode and its electrochemical application. Electrochem Commun 13:133–137. https://doi.org/10.1016/j.elecom.2010.11.033

Chen H, Cui C, Ma X, Yang W, Zuo Y (2020) Amperometric biosensor for *Brucella* testing through molecular orientation technology in combination with signal amplification technology. ChemElectroChem. 7(12):2672–2679

Dca B, Fan DB, Xue ZB, Bq A, Xw B, Kz B (2022) A universal constructing method for high performance DNA biosensors based on the optimized photoelectrode material and dual recycling amplification. Appl Surf Sci 585:152661

De Lima LF, Pereira EA, Ferreira M (2020) Electrochemical sensor for propylparaben using hybrid Layer-by-Layer films composed of gold nanoparticles, poly (ethylene imine) and nickel (II) phthalocyanine tetrasulfonate. Sens Actuators, B Chem 310:127893. https://doi.org/10.1016/j.snb.2020.127893

Dk YENİ, Doğan A (2021) Evaluation of the analytical efficiency of Real-Time PCR in the diagnosis of Brucellosis in cattle and sheep. Kafkas Üniversitesi Veteriner Fakültesi Dergisi 27:503–509

Dong XX, Wang Y, Shen YD, Sun MY, Wang H, Lei HT, Xiao ZL, Yang JY, Xu ZL (2015) Nano material based novel electrochemical immunosensor and its application in the field of food safety. J Chinese Inst Food Sci Technol 15:136–146. https://doi.org/10.16429/j.1009-7848.2015.04.019

Gao J, Wang C, Chu Y, Han Y, Gao Y, Wang Y, Zhang Y (2022a) Graphene oxide-graphene Van der Waals heterostructure transistor biosensor for SARS-CoV-2 protein detection. Talanta 240:123197

Gao S, Guisán JM, Rocha-Martin J (2022b) Oriented immobilization of antibodies onto sensing platforms-A critical review. Anal Chim Acta 1189:338907

Guang-Feng W, Yan-Hong Z, Ling C, Lun W (2013) Applications of functional nanomaterials in electrochemical immunosensor. Chin J Analy Chem 41(4):608–615

Hezard T, Fajerwerg K, Evrard D, Collière V, Behra P, Gros P (2012) Gold nanoparticles electrodeposited on glassy carbon using cyclic voltammetry: Application to Hg (II) trace analysis. J Electroanal Chem 664:46–52. https://doi.org/10.1016/j.jelechem.2011.10.014

Huang S, Si Z, Li X, Zou J, Yao Y, Weng D (2016) A novel Au/r-GO/TNTs electrode for H2O2, O2 and nitrite detection. Sens Actuators, B Chem 234:264–272. https://doi.org/10.1016/j.snb.2016.04.167

Jafari-Kashi A, Rafiee-Pour HA, Shabani-Nooshabadi M (2022) A new strategy to design label-free electrochemical biosensor for ultrasensitive diagnosis of CYFRA 21–1 as a biomarker for detection of non-small cell lung cancer. Chemosphere 301:134636

Khan S, Ansari ZA, Alothman OY, Fouad H, Ansari SG (2017) Application of amine and copper doped magnesium oxide nanoparticles in electrochemical immunosensors for detecting *Brucella* abortus. Nanosci Nanotechnol Lett 9(11):1656–1664

Khan S, Ansari ZA, Seo HK, Ansari SG (2018) Synthesis and application of Cu-doped nickel and zirconium oxide nanoparticles as *Brucella* abortus electrochemical device development. Sens Lett 16(4):267–276

Li Y, Tang DP (2011) Graphene oxide- thionine and gold nanoparticles- functionalized amperometric biosensor for determination of glucose. J Fuzhou Univ (Natural Science Edition) 39:781–785

Liu S, Haller E, Horak J, Brandstetter M, Heuser T, Lämmerhofer M (2019) Protein A-and Protein G-gold nanoparticle bioconjugates as nano-immunoaffinity platform for human IgG depletion in plasma and antibody extraction from cell culture supernatant. Talanta 194:664–672. https://doi.org/10.1016/j.talanta.2018.10.079

Love JC, Estroff LA, Kriebel JK, Nuzzo RG, Whitesides GM (2005) Self-assembled monolayers of thiolates on metals as a form of nanotechnology. Chem Rev 105:1103–1170. https://doi.org/10.1021/cr0300789

Malathi S, Pakrudheen I, Kalkura SN, Webster TJ, Balasubramanian S (2022) Disposable biosensors based on metal nanoparticles. Sens Int 3:100169

Moon J, Byun J, Kim H, Jeong J, Lim EK, Jung J, Cho S, Cho WK, Kang T (2019) Surface-independent and oriented immobilization of antibody via one-step polydopamine/protein g coating: application to influenza virus immunoassay. Macromol Biosci 19(6):1800486

Pérez-Fernández B, de la Escosura Muñiz A (2022) Electrochemical biosensors based on nanomaterials for aflatoxins detection: a review (2015–2021). Anal Chim Acta 1212:339658

Robi DT, Gelalcha BD (2020) Epidemiological investigation of brucellosis in breeding female cattle under the traditional production system of Jimma zone in Ethiopia. Veterinary Animal Sci 9:100117. https://doi.org/10.1016/j.vas.2020.100117

Sabour S, Arzanlou M, Jeddi F, Azimi T, Hosseini-Asl S, Naghizadeh-Baghi A, Peeri Dogaheh H (2020) Evaluating the efficiency of TaqMan real-time PCR and serological methods in the detection of Brucella spp. in clinical specimens collected from suspected patients in Ardabil, Iran. J Microbiol Methods 175:105982

Satei E, Mirshahabi H, Zeighami H, Gholoobic A, Sadeghi H (2020) Molecular survey of BCSP31 and IS711 using PCR assays in detection of Brucella spp. in raw milk. Meta Gen 24:100683

Smith KCA, Oatley CW (1955) The scanning electron microscope and its fields of application. Bri J Appl Phys 6(11):391

Ulman A (1996) Formation and structure of self-assembled monolayers. Chem Rev 96(4):1533–1554. https://doi.org/10.1021/cr9502357

Wahab R, Khan ST, Ahmad J, Musarrat J, Al-Khedhairy AA (2017) Functionalization of anti-*Brucella* antibody on ZnO-NPs and their deposition on aluminum sheet towards developing a sensor for the detection of *Brucella*. Vacuum 146:592–598. https://doi.org/10.1016/j.vacuum.2017.01.019

Wang AJ, Zhu XY, Chen Y, Yuan PX, Luo X, Feng JJ (2019) A label-free electrochemical immunosensor based on rhombic dodecahedral Cu3Pt nanoframes with advanced oxygen reduction performance for highly sensitive alpha-fetoprotein detection. Sens Actuators B Chem 288:721–727

Wang Z, Yang S, Wang Y, Feng W, Li B, Jiao J, Han B, Chen Q (2020) A novel oriented immunosensor based on AuNPs-thionine-CMWCNTs and staphylococcal protein A for interleukin-6 analysis in complicated biological samples. Anal Chim Acta 1140:145–152. https://doi.org/10.1016/j.aca.2020.10.025

Wu H, Zuo Y, Cui C, Yang W, Ma H, Wang X (2013) Rapid quantitative detection of *Brucella* melitensis by a label-free impedance immunosensor based on a gold nanoparticle-modified screen-printed carbon electrode. Sensors. 13(7):8551–8563

Yin YY, Hou L, Zhang LL, Lin XB, Wu XP (2018) Electrochemical Immunosensor for Microcystin-LR Detection Based on Nanocomposite Material Immobilization and Enzymatic Amplification. Chin J Anal Chem 46:493–501. https://doi.org/10.11895/j.issn.0253-3820.171055

Yin CX (2019) Preparation of electrochemical biosensors based on gold nanocomposites and their application, Qingdao University of Science and Technology.

Yuan YF (2014) A study of the characteristics of X-ray technology applications and their current development. J yan'an Vocational Tech Inst 28:123–124

Yuan Q, He J, Niu Y, Chen J, Zhao Y, Zhang Y, Yu C (2018) Sandwich-type biosensor for the detection of α2, 3-sialylated glycans based on fullerene-palladium-platinum alloy and 4-mercaptophenylboronic acid nanoparticle hybrids coupled with Au-methylene blue-MAL signal amplification. Biosens Bioelectro 102:321–327

Zhang SJ, Kang WJ, Niu LM (2019) Electrochemical behavior of dopamine at a biosensor based on a composite of gold nanoparticles and graphene, and its application in dopamine determination. Chem Res Appl. https://doi.org/10.3969/j.issn.1004-1656.2019.09.003

Zhang M, Ding Q, Zhu M, Yuan R, Yuan Y (2022) An ultrasensitive electrochemical biosensor with amplification of highly efficient triple catalytic hairpin assembly and tetris hybridization chain reaction. Sens Actuators, B Chem 361:131683

Zhao Z, Sun Y, Li P, Sang S, Zhang W, Hu J, Lian K (2014) A sensitive hydrazine electrochemical sensor based on zinc oxide nano-wires. J Electrochem Soc 161:B157. https://doi.org/10.1149/2.095406jes

Zhao G, Zhou B, Wang X, Shen J, Zhao B (2021) Detection of organophosphorus pesticides by nanogold/mercaptomethamidophos multi-residue electrochemical biosensor. Food Chem 354:129511